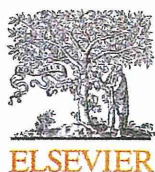


- [4] Y. Ichijima, K. Yoshioka, Y. Yoshioka, K. Shinohe, H. Fujimori, J. Unno, M. Takagi, H. Goto, M. Inagaki, S. Mizutani, H. Teraoka, DNA lesions induced by replication stress trigger mitotic aberration and tetraploidy development, *PLoS One* 5 (2010) e8821.
- [5] A. Matheu, A. Maraver, P. Klatt, I. Flores, I. Garcia-Cao, C. Borrás, J.M. Flores, J. Vina, M.A. Blasco, M. Serrano, Delayed ageing through damage protection by the Arf/p53 pathway, *Nature* 448 (2007) 375–379.
- [6] K. Yoshioka, Y. Atsumi, H. Fukuda, M. Masutani, H. Teraoka, The quiescent cellular state is Arf/p53-dependent and associated with H2AX downregulation and genome stability, *International Journal of Molecular Sciences* 13 (2012) 6492–6506.
- [7] Y. Atsumi, H. Fujimori, H. Fukuda, A. Inase, K. Shinohe, Y. Yoshioka, M. Shikanai, Y. Ichijima, J. Unno, S. Mizutani, N. Tsuchiya, Y. Hippo, H. Nakagama, M. Masutani, H. Teraoka, K. Yoshioka, Onset of quiescence following p53 mediated down-regulation of H2AX in normal cells, *PLoS One* 6 (2011) e23432.
- [8] C.A. Brady, D. Jiang, S.S. Mello, T.M. Johnson, L.A. Jarvis, M.M. Kozak, D. Keenzelmann Broz, S. Basak, E.J. Park, M.E. McLaughlin, A.N. Karnezis, L.D. Attardi, Distinct p53 transcriptional programs dictate acute DNA-damage responses and tumor suppression, *Cell* 145 (2011) 571–583.
- [9] T. Li, N. Kon, L. Jiang, M. Tan, T. Ludwig, Y. Zhao, R. Baer, W. Gu, Tumor suppression in the absence of p53-mediated cell-cycle arrest, apoptosis, and senescence, *Cell* 149 (2012) 1269–1283.
- [10] L.A. Donehower, M. Harvey, B.L. Slagle, M.J. McArthur, C.A. Montgomery Jr., J.S. Butel, A. Bradley, Mice deficient for p53 are developmentally normal but susceptible to spontaneous tumours, *Nature* 356 (1992) 215–221.
- [11] T. Kamijo, F. Zindy, M.F. Roussel, D.E. Quelle, J.R. Downing, R.A. Ashmun, G. Grosveld, C.J. Sherr, Tumor suppression at the mouse INK4a locus mediated by the alternative reading frame product p19ARF, *Cell* 91 (1997) 649–659.
- [12] D.A. Liebermann, B. Hoffman, D. Vesely, P53 induced growth arrest versus apoptosis and its modulation by survival cytokines, *Cell Cycle* 6 (2007) 166–170.
- [13] C. Lu, W.S. El-Deiry, Targeting p53 for enhanced radio- and chemo-sensitivity, *Apoptosis: An International Journal on Programmed Cell Death* 14 (2009) 597–606.
- [14] H.F. Ding, D.E. Fisher, Mechanisms of p53-mediated apoptosis, *Critical Reviews in Oncogenesis* 9 (1998) 83–98.
- [15] S.D. Tyner, S. Venkatachalam, J. Choi, S. Jones, N. Ghebranious, H. Igelmann, X. Lu, G. Soron, B. Cooper, C. Brayton, S.H. Park, T. Thompson, G. Karsenty, A. Bradley, L.A. Donehower, P53 mutant mice that display early ageing-associated phenotypes, *Nature* 415 (2002) 45–53.
- [16] B. Maier, W. Gluba, B. Bernier, T. Turner, K. Mohammad, T. Guise, A. Sutherland, M. Thorner, H. Scoble, Modulation of mammalian life span by the short isoform of p53, *Genes & Development* 18 (2004) 306–319.
- [17] G.W. Hinkal, C.E. Gatzka, N. Parikh, L.A. Donehower, Altered senescence, apoptosis, and DNA damage response in a mutant p53 model of accelerated aging, *Mechanisms of Ageing and Development* 130 (2009) 262–271.
- [18] O.A. Sedelnikova, I. Horikawa, D.B. Zimonjic, N.C. Popescu, W.M. Bonner, J.C. Barrett, Senescing human cells and ageing mice accumulate DNA lesions with unreparable double-strand breaks, *Nature Cell Biology* 6 (2004) 168–170.
- [19] W.M. Bonner, C.E. Redon, J.S. Dickey, A.J. Nakamura, O.A. Sedelnikova, S. Solier, Y. Pommier, GammaH2AX and cancer, *Nature Reviews Cancer* 8 (2008) 957–967.
- [20] C.H. Bassing, F.W. Alt, H2AX may function as an anchor to hold broken chromosomal DNA ends in close proximity, *Cell Cycle* 3 (2004) 149–153.
- [21] D.R. Pilch, O.A. Sedelnikova, C. Redon, A. Celeste, A. Nussenzweig, W.M. Bonner, Characteristics of gamma-H2AX foci at DNA double-strand breaks sites, *Biochemistry and Cell Biology* 81 (2003) 123–129.
- [22] O. Fernandez-Capetillo, A. Lee, M. Nussenzweig, A. Nussenzweig, H2AX: the histone guardian of the genome, *DNA Repair* 3 (2004) 959–967.
- [23] K. Yoshioka, Y. Yoshioka, P. Hsieh, ATR kinase activation mediated by MutSalpha and MutLalpha in response to cytotoxic O6-methylguanine adducts, *Molecular Cell* 22 (2006) 501–510.
- [24] G.J. Todaro, H. Green, Quantitative studies of the growth of mouse embryo cells in culture and their development into established lines, *The Journal of Cell Biology* 17 (1963) 299–313.
- [25] S.W. Lowe, T. Jacks, D.E. Housman, H.E. Rulley, Abrogation of oncogene-associated apoptosis allows transformation of p53-deficient cells, *Proceedings of the National Academy of Sciences of the United States of America* 91 (1994) 2026–2030.
- [26] I.H. Lee, Y. Kawai, M.M. Fergusson, I.I. Rovira, A.J. Bishop, N. Motoyama, L. Cao, T. Finkel, Atg7 modulates p53 activity to regulate cell cycle and survival during metabolic stress, *Science* 336 (2012) 225–228.
- [27] T.A. Chan, H. Hermeking, C. Lengauer, K.W. Kinzler, B. Vogelstein, 14-3-3Sigma is required to prevent mitotic catastrophe after DNA damage, *Nature* 401 (1999) 616–620.
- [28] I. Vitale, L. Galluzzi, M. Castedo, G. Kroemer, Mitotic catastrophe: a mechanism for avoiding genomic instability, *Nature Reviews Molecular Cell Biology* 12 (2011) 385–392.
- [29] M. Zajac, M.V. Moneo, A. Carnero, J. Benitez, B. Martínez-Delgado, Mitotic catastrophe cell death induced by heat shock protein 90 inhibitor in BRCA1-deficient breast cancer cell lines, *Molecular Cancer Therapeutics* 7 (2008) 2358–2366.
- [30] J.B. Stevens, G. Liu, S.W. Bremer, K.J. Ye, W. Xu, J. Xu, Y. Sun, G.S. Wu, S. Savasan, S.A. Krawetz, C.J. Ye, H.H. Heng, Mitotic cell death by chromosome fragmentation, *Cancer Research* 67 (2007) 7686–7694.
- [31] J. Portugal, S. Mansilla, M. Bataller, Mechanisms of drug-induced mitotic catastrophe in cancer cells, *Current Pharmaceutical Design* 16 (2010) 69–78.
- [32] H. Fujimori, M. Shikanai, H. Teraoka, M. Masutani, K. Yoshioka, Induction of cancerous stem cells during embryonic stem cell differentiation, *The Journal of Biological Chemistry* 287 (2012) 36777–36791.



Poly(ADP-ribosylation) regulates chromatin organization through histone H3 modification and DNA methylation of the first cell cycle of mouse embryos

Tomoharu Osada^{a,b,*}, Anna-Margareta Rydén^c, Mitsuko Masutani^{c,*}

^aAdvanced Medical Science Research Department, Mitsubishi Chemical Medience Corporation, 14-1 Sunayama, Kamisu-shi, Ibaragi 314-0255, Japan

^bDepartment of Regenerative and Developmental Biology, Mitsubishi Kagaku Institute of Life Sciences (MILS), 11 Minamiooya, Machida-shi, Tokyo 194-8511, Japan

^cDivision of Genome Stability Research, National Cancer Center Research Institute, 5-1-1 Tsukiji, Chuo-ku, Tokyo 104-0045, Japan

ARTICLE INFO

Article history:

Received 3 March 2013

Available online 30 March 2013

Keywords:

Fertilization

Histone modification

DNA methylation

Poly(ADP-ribosylation)

Post-translational modification

ABSTRACT

We examined the roles of poly(ADP-ribosylation) in chromatin remodeling during the first cell cycle of mouse embryos. Drug-based inhibition of poly(ADP-ribosylation) by a PARP inhibitor, PJ-34, revealed up-regulation of dimethylation of histone H3 at lysine 4 in male pronuclei and down-regulation of dimethylation of histone H3 at lysine 9 (H3K9) and lysine 27 (H3K27). Association of poly(ADP-ribosylation) with histone modification was suggested to be supported by the interaction of Suz12, a histone methyltransferase in the polycomb complex, with Parp1. PARP activity was suggested to be required for a proper localization and maintenance of Suz12 on chromosomes. Notably, DNA methylation level of female pronuclei in one-cell embryos was robustly decreased by PJ-34. Electron microscopic analysis showed a frequent appearance of unusual electron-dense areas within the female pronuclei, implying the disorganized and hypercondensed chromatin ultrastructure. These results show that poly(ADP-ribosylation) is important for the integrity of non-equivalent epigenetic dynamics of pronuclei during the first cell cycle of mouse embryos.

© 2013 Elsevier Inc. All rights reserved.

1. Introduction

Poly(ADP-ribosylation) (PARylation) is an instant posttranslational modification of protein and is involved in many cellular processes [1,2]. In particular, recent studies have revealed its essential roles in chromatin remodeling for transcription [3–6]. Modification of PARylation triggers loosening of chromatin structure, which enables the access of transcriptional factors to the DNA duplex structure. In addition, poly(ADP-ribose) polymerase (PARP) is localized mainly on chromatin of transcriptionally active genes, which are clearly segregated from the localization of histone H1 on transcriptionally-suppressed genes [7]. However, it is not clear how PARylation affects transcription-independent chromatin remodeling of the first cell cycle of mouse development.

During the first cell cycle of mouse embryos, a few genes are transcribed mainly from paternal genome [8,9]. Inhibition of transcription during one-cell embryos by RNA polymerase inhibitors showed the dispensable roles of RNA polymerases at the beginning

of mouse development [10]. However, zygotic gene activation is required for progression from 2-cell to 4-cell embryos [11,12]. These findings indicate that posttranslational regulation of protein should act as a stem mechanism of the development of one-cell embryos. Upon fertilization, highly compacted chromatin of gametes was acutely decondensed to form pronuclei within a few hours. Protamines of sperm chromatin are replaced by maternal histone H1 during this process, which may be associated with global DNA hypomethylation of sperm-derived pronuclei (PN) [13,14]. In contrast, maternal chromatin arrested at metaphase II progressed rapidly into G1 phase and subsequently forms the female PN. DNA synthesis from paternal genome is preceded to that from maternal DNA. A minor transcription is activated solely from male pronuclei. This evidence suggests that the requirement for the posttranslational regulations of parental genomes before mingling of both gamete DNA to begin the proper zygotic development.

Of posttranslational modification of proteins, we examined here the effects of PARylation during the first cell cycle of mouse embryos, because metabolism of NAD, which is the substrate of PARPs, is acutely activated upon fertilization [15,16]. We previously showed that PARP inhibitor blocked pronuclear fusion at pronuclear envelop breakdown, with defective polymerization of tubulins, reduced MAPK signaling, and decreased phosphorylation of lamin A/C [17,18]. However, the role of PARylation in chromatin regulation in one-cell embryos is yet to be elucidated. Here we further studied the functions of PARylation in non-equivalent

* Corresponding authors. Address: Advanced Medical Science Research Department, Mitsubishi Chemical Medience Corporation, 14-1 Sunayama, Kamisu-shi, Ibaragi 314-0255, Japan (T. Osada), Division of Genome Stability Research, National Cancer Center Research Institute, 5-1-1 Tsukiji, Chuo-ku, Tokyo 104-0045, Japan (M. Masutani).

E-mail addresses: osada.tomoharu@mg.medience.co.jp (T. Osada), mmasutani@ncc.go.jp (M. Masutani).

chromatin dynamics of pronuclei and epigenetic regulation in the first cell cycle of mouse embryos.

2. Materials and methods

2.1. Oocyte and embryo manipulations

Parp1^{-/-} mutant mice [19] with a B6D2F1 hybrid or C57BL/6J inbred background were used in this study. Oocytes were collected from the superovulated B6D2F1 females 14 hrs after the intraperitoneal injection of pregnant mare serum gonadotropin (PMSG), followed by the injection of human chorionic gonadotropin (hCG). For in vitro fertilization using TYH medium [20], sperm was collected from the caudal epididymis of B6D2F1 males and incubated in TYH medium for at least 30 min for the hyperactivation. The oocyte-cumulus complexes (OCC) were collected from the ampulla of uterine tube of superovulated mice. Sperm (150 sperm/ μ l) were inseminated in the OCC-containing TYH medium with or without PJ-34 (N-(6-Oxo-5,6-dihydro-phenanthridin-2-yl)-N,N-dimethylacetamide, Alexis Biochemicals) or 5-AIQ (5-aminoisoquinolin-1(2H)-one, Alexis Biochemicals). Intracytoplasmic sperm injection (ICSI) was carried out essentially as described previously [21]. ICSI was carried out in HEPES-buffered CZB medium [22] with or without 30 μ M PJ-34. Thereafter, embryos were cultured in modified Whitten medium [23].

2.2. Antibodies

The antibodies and dilutions used in this study are described in Supplemental Table T1. The HRP-conjugated rat or rabbit IgG (1:10,000, Jackson ImmunoResearch Laboratory) and HRP-conjugated mouse IgG (1:1000, Bio-RAD) were used as the secondary antibodies and the Alex Fluor conjugates (1:200, Invitrogen) of IgG for immunofluorescence.

2.3. Immunofluorescence

The cumulus-oocyte complex was dissociated by hyaluronidase (Sigma) and the zona pellucida was removed with 0.5% actinase (Kaken, Japan). After incubation of the denuded oocytes or embryos for at least 30 min, the oocytes or embryos were placed into fibrin clots [24]. The fibrin clots were prepared by mixing 1 μ l fibrinogen (Calbiochem) with 1 μ l thrombin (Sigma). The cells were incubated with primary antibodies for overnight at 4 °C, followed by incubation with blocking buffer (PBS containing 5% normal goat serum and 0.05% Tween-20). The cells were then incubated with secondary antibodies for 1–2 h at 37 °C. After washing with PBS, the cells were counterstained with PI and subjected to microscopic analyses. For the staining of histone modification antibodies, the cells were fixed with 4% paraformaldehyde for 15 min at 4 °C and then permeabilized with PBS containing 0.1% BSA and 0.5% TritonX-100 for 10 min. An immunofluorescence study using 12 kinds of histone acetylation and methylation antibodies was initially carried out using 7–10 embryos to determine the optimum reaction conditions for each antibody. The cells were incubated with primary antibodies overnight at 4 °C, and then with secondary antibodies for at least 3 h at 4 °C. For the staining of DNA methylation, after fixation and permeabilization as described above, embryos were incubated with 2 M HCl for 45 min and then neutralized for 10 min with 100 mM Tris/HCl buffer, pH 8.5. After washing five times with PBS containing 0.05% Tween-20, the embryos were blocked and incubated with anti-5-methylcytosine antibody overnight and incubated with secondary antibody as described above. The DNA was counterstained with DAPI or PI. The images were captured under a light microscopy (Axiophot, Zeiss)

or confocal microscopy (IX71 with Fluoview FV300, Olympus) system.

2.4. Two-hybrid screening

Yeast two-hybrid screening was performed with Matchmaker GAL4 Two-hybrid System 3 (Clontech), according to the manufacturer's instructions. Briefly, the cDNA fragments of Δ *Parp1* (encoding amino acids 1–739, accession number, NM_007415) were generated by PCR amplification with appropriate primer sequences (Forward, 5'-TGCAGCAGGAGAAGGAGG-3'; Reverse, 5'-GTTGAC-GTCGATGGGATCC-3'). Template cDNA was synthesized from mRNA of mouse ovary or brain using SuperScript III (Invitrogen). The Δ *Parp1* was then cloned into the vector pGBKT7. To prepare the cDNA library from MII oocytes, the total RNA was isolated from 100 MII oocytes with Sepasol (Nacalai) according to the manufacturer's instructions. The MII oocyte-derived cDNA was cloned into pGADT7 and bait vectors were co-transfected into the competent yeast strain AH109. The cDNA clones were recovered from nutritionally selected yeast colonies. Confirmation of the interactions in yeast was carried out by co-transfection of the bait vectors and isolated pGADT7 clones (Supplemental Table T2).

2.5. Plasmid preparation and immunoprecipitation

The full-length cDNA encoding Suz12 (NM_199196) was amplified by PCR from cDNA pools derived from mouse ovary or brain (Forward, 5'-GGCCATGGAGGCCACCATGGCGCCTCAGAAGCAC-3'; Reverse, 5'-GGTACCTCAGAGTTTTGTTCTTGC-3'). The full-length cDNA encoding Suz12 and Δ *Parp1* were cloned into the pCMV-HA and pCMV-Myc mammalian expression vectors (Clontech), respectively. The plasmids were transfected into COS or HEK293T cells by Polyfect transfection reagent (Qiagen), Lipofectamine 2000 (Invitrogen), or the Profection mammalian transfection system (Promega), according to manufacturers' instructions. Forty to 48 h after transfection, the cells were collected into IP lysis buffer (150 mM NaCl, 1% NP-40, 50 mM Tris-HCl (pH 7.5)) or a commercially available lysis buffer (MER buffer (Pierce)), and the lysates were kept at –80 °C. Immunoprecipitation was carried out using the Profound™ Mammalian HA/c-Myc Tag Co-IP kit (Pierce) according to the manufacturer's instructions, or agarose conjugated anti-epitope tag antibodies (MBL). After primary immunoprecipitation with anti-myc agarose, the immunocomplexes were eluted with an elution buffer (pH 2.8, provided by Pierce) and immediately equilibrated with 10 mM Tris-HCl (pH 9.5). Western blots were performed using primary antibodies after SDS-polyacrylamide gel electrophoresis and transfer to Immobilon PVDF membrane (Millipore). Briefly, the membrane was reacted with primary antibodies overnight at 4 °C. The membrane was washed and then incubated with secondary HRP-conjugated antibodies for 2 h at room temperature. The signals were detected with the Chemi-Lumi One kit (Nacalai).

3. Results

3.1. Effects of PARylation on histone modification of the PN embryos

We first examined the effects of PARylation on chromatin modification during postfertilization development using PARP inhibitor PJ-34, because our previous study showed that PJ-34 blocked pronuclear fusion at pronuclear envelop breakdown [17]. In the absence of PJ-34 (untreated embryos), dimethylation of histone H3 at lysine 4 (dimethyl-H3K4) was only observed in the female pronuclei and not in the male pronuclei at 6 h post fertilization (hpf). An upregulation of dimethyl-H3K4 in the male pronuclei at 6 hpf

was detected in the presence of PJ-34 (Fig. 1). The levels of dimethyl-H3K9 were detected in both pronuclei, but down-regulated in both pronuclei in the presence of PJ-34. The level of dimethyl-H3K27 was dominantly observed in female pronuclei at 6 hpf (data not shown) and 15 hpf in the untreated embryos. In contrast, dimethyl-H3K27 was downregulated in the parental pronuclei of PJ-34-treated embryos at 15 hpf (Fig. 1). Western blots also show the upregulation of dimethyl-H3K4 in the PARylation-inhibited embryos at 6 hpf, and downregulation of dimethyl-H3K9 and dimethyl-H3K27 at 15 hpf in the presence of PJ-34 (Fig. 1).

3.2. Physical interaction of Parp1 with Suz12

To elucidate the molecular basis of the effect of PARylation on histone modification, we performed yeast two-hybrid screening using the bait vector carrying the N-terminal and automodification domain of Parp-1, which is the major protein-protein interaction domain, but is lacking the catalytic domain (Δ Parp1), because no interactants were obtained through two trials using intact Parp1 bait proteins (data not shown), which may result from ectopic

expression/activation of Parp1 toxic in yeast as previously described [25]. Twelve protein candidates interacting with Parp1 were identified (Supplemental Table T2). Among these molecules, we focused on Suz12, a histone methyltransferase in PRC2/3/4 (Polycomb Repressive Complex 2/3/4). Suz12 induces an inactive state of chromatin by modifying histone H3K9 and H3K27 residues. A reciprocal immunoprecipitation study further confirmed the direct interaction of Suz12 with Δ Parp1 in HEK293T cells (Fig. 2A).

Immunofluorescence analysis showed Suz12 localized prominently on the spindle of MII oocytes as well as in the ooplasm (Fig. 2B). Notably, in the MII oocytes treated with PJ-34, the signals of Suz12 were hardly detected (Fig. 2D), indicating a possibility that Suz12 may not be stable under deficient PARylation condition. After fertilization, at 6 hpf, Suz12 was mainly detected in both pronuclei, like PAR molecules [17] in the absence of PJ-34 (Fig. 2C). We previously reported that in this stage, Parp1 is localized in pronuclei as well as in ooplasm [17]. PJ-34 treatment disturbed pronuclear fusion as previously reported [17] and reduced the Suz12 immunosignals in the pronuclei and the localization of the

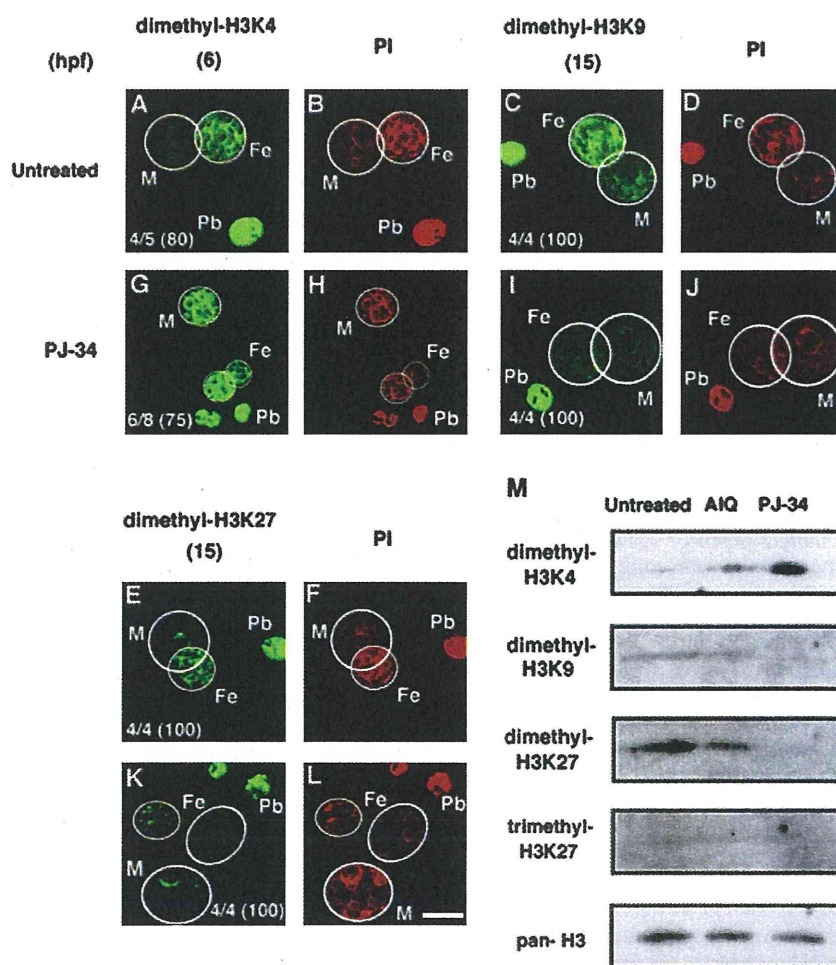


Fig. 1. Analysis of histone modification under PARylation inhibition at the one-cell mouse embryos. Immunofluorescence study with laser-scanning confocal microscopy of untreated (A–F) or 30 μ M PJ-34 treated (G–L) one-cell embryos at 6 hpf was performed with antibodies for dimethylated histone H3 at lysine 4 (dimethyl-H3K4), dimethylated histone H3 at lysine 9 (dimethyl-H3K9), dimethylated histone H3 at lysine 27 (dimethyl-H3K27), and is depicted in green. The frequency of the staining patterns and its percentage is given in parenthesis in white (A, C, E, G, I, K). DNA was counterstained with PI (B, D, F, H, J, L). Female (Fe) and male (M) pronuclei (PN), and the nuclei of polar body (Pb) are indicated. Circles (white lines) indicate the outlines of PN. (M) Western blots were performed with crude extracts corresponding to 100 PN embryos with antibodies against dimethyl-H3K4, dimethyl-H3K9, dimethyl-H3K27, trimethylated histone H3 at lysine 27 (trimethyl-H3K27), and unmodified histone H3 (pan-H3). Bar represents 25 μ m. (For interpretation of color in Figure, the reader is referred to the web version of this article).

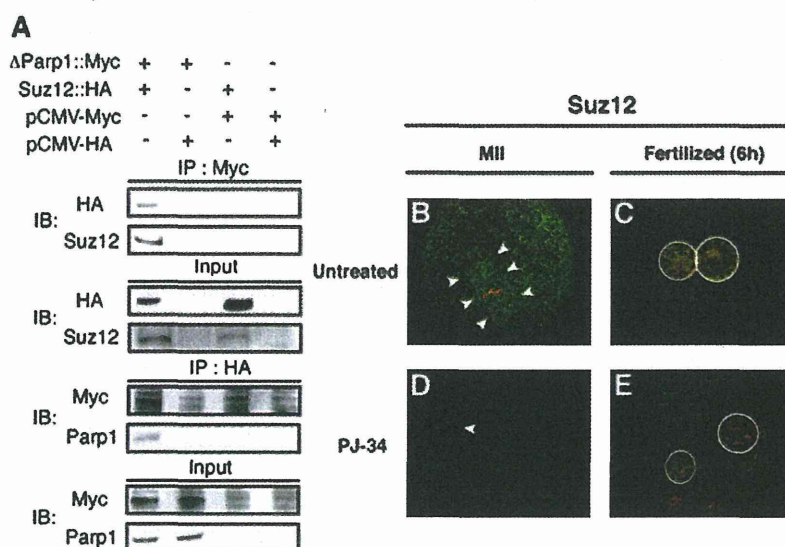


Fig. 2. Interaction of Parp1 with Suz12 in vitro and localization of Suz12 in the PN of mouse one-cell embryos. Extracts from HEK293T cells transfected with combinations of plasmids carrying mouse Parp1 lacking the catalytic domain (Δ Parp1) tagged with Myc (Δ Parp1::Myc), intact Suz12 tagged with HA (Suz12::HA), and mock plasmids (CMV-Myc, CMV-HA) were used for immunoprecipitation (IP) followed by immunoblotting (IB) (A). Immunofluorescence study of MII oocytes (B and D), or one-cell embryos at 6 hpf (C and E). Detected antigens appear green. DNA counterstained by PI is colored with red. Merged signals appear yellow or orange. Arrowheads indicate the spindle structure (B) and MII chromosome (D) positive for the anti-Suz12 antibody. White circle represents the outline of pronuclei (C and E). The frequency (percentage in parenthesis) of staining patterns was indicated in each panel (B–E). Bar represents 10 μ m. (For interpretation of color in Figure, the reader is referred to the web version of this article).

immunosignals in the ooplasm is slightly increased (Fig. 2E). These results suggest that PARylation is required for proper localization of Suz12 on the chromosomes during the pronuclei fusion period.

3.3. Hypomethylation of maternal gamete DNA by PARylation inhibition

Recently, functional links between histone methylation and DNA methylation have been elucidated [26,27]. We next sought for the roles of PARylation in DNA methylation. Global methylation of the maternal genome is maintained and sperm DNA is quickly demethylated during the postfertilization period [28]. Through our immunofluorescence study we detected signals of 5-methylcytosine (MetC) in the female pronuclei of embryos produced by in vitro fertilization (IVF) and both pronuclei of parthenogenetic embryos at 6 hpf/post-activation (hpa), as well as the nuclei of the polar bodies (Fig. 3A and B). By incubation with PJ-34, the MetC-immunoreactivity became almost absent in both pronuclei of IVF and parthenogenetic embryos (Fig. 3C and D), indicating the robust hypomethylation of female pronuclei. The low immunoreactivity to the MetC antibody in the PJ-34 treated embryos persisted at least until 15 hpf with PJ-34 in the culture medium (data not shown). These results indicate that PARylation is involved in the maintenance of global DNA methylation of female pronuclei.

3.4. Disorganized chromatin ultrastructure under PARylation inhibition in the pronuclei

We further investigated the chromatin organization of the pronuclei and effects by PARylation inhibition by electron microscopy (EM). Rosette-like structure of electron-dense areas was detected in the female pronuclei of untreated one-cell embryos at 6 and 15 hpf (Fig. 3). Such electron-dense areas were not detected in male pronuclei at 6 hpf but appeared at 15 hpf (Fig. 3I–K). With PJ-34 treatment, electron-dense areas are increasingly detectable in the female pronuclei, but not in the male pronuclei at 6 hpf

(Fig. 3K–T). At 15 hpf, uncharacterized structure with a high electron-density was observed in female pronuclei and the electron-dense areas became increasingly detectable also in the male pronuclei in the presence of PJ-34 (Fig. 2S and T). It is thus suggested that PARylation inhibition induces rosette-like electron-dense areas corresponding to disorganized hypercondensed chromatin in the pronuclei.

4. Discussion

This study shows that PARylation regulates methylation of histone H3 and DNA methylation during the first cell cycle of mouse development. Furthermore, our data suggests that PARylation is important for the integrity of non-equivalent chromatin organization of the pronuclei of one-cell embryos.

Our observation of global upregulation of dimethyl-H3K4 and downregulation of both dimethyl-H3K9 and dimethyl-H3K27 suggests that chromatin modification during the first cell-cycle seems to shift toward global transcription activation under a normal development (Fig. 4). This mechanism should be important for genome-wide transcriptional upregulation, but is likely not important for transcription of a limited number of genes expressed at the one-cell embryos, whose expression is indispensable for further development. We speculate that PARylation is required for proper conversion of parental genomes during one-cell stage prior to the global activation of the zygotic genome that takes place at the two-cell stage. Roles of PARylation in histone modification regulation have been shown to involve both transcription and replication [29,30] as well as DNA repair and recombination [31]. In addition, PARylation affects relaxation of chromatin structure in vitro [32] and in vivo [33], which may be mediated by PARylation of Parp1 itself or histone H1. Our findings provide a unique biological window to elucidate the regulation of PARylation on chromatin ultrastructure in mammalian development (Fig. 4).

Our findings also demonstrate that PARylation acts as regulatory machinery for the methylation of histone H3 (Fig. 4). Aberrant

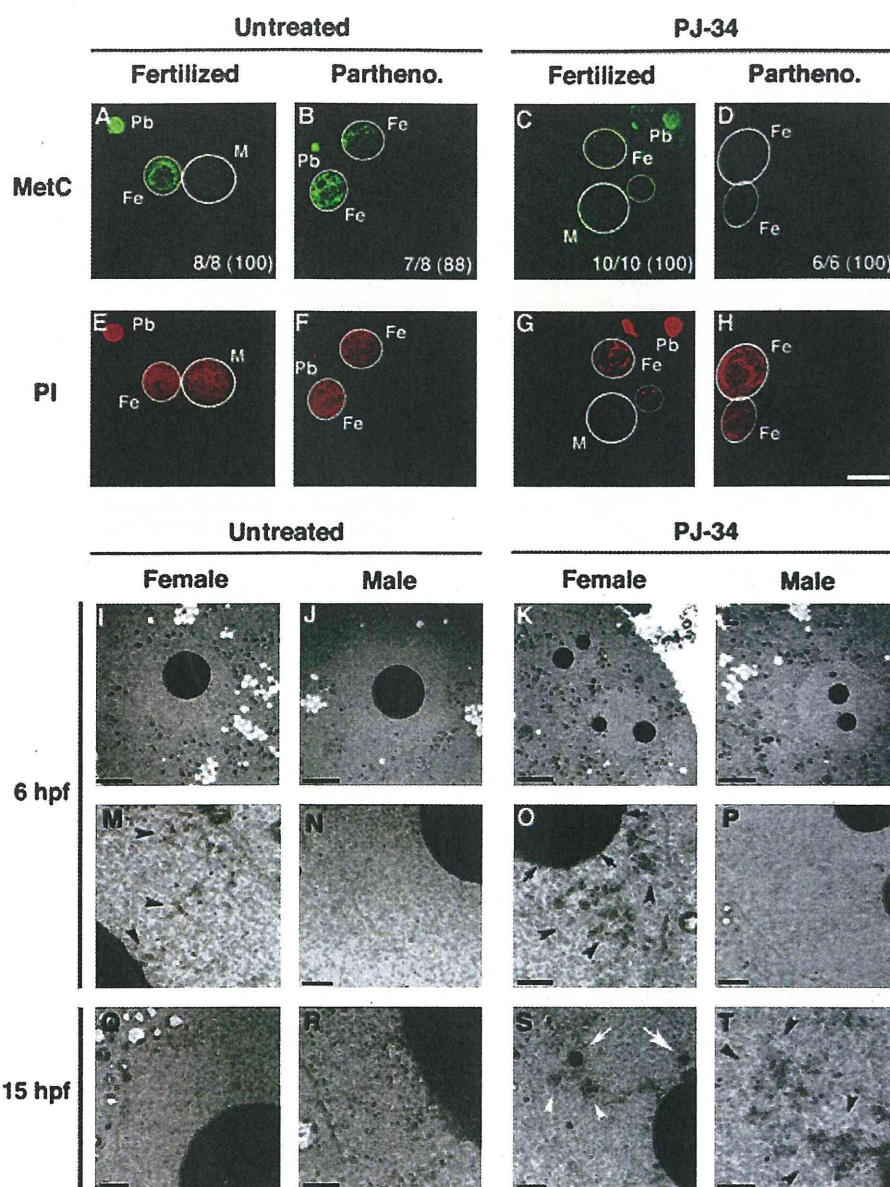


Fig. 3. Effects of PARylation inhibition on DNA methylation and ultrastructure of pronuclear organization by electron microscopy. Laser scanning confocal immunofluorescence study using IVF (fertilized; A and C) and parthenogenetic (parthenotes; B and D) embryos at 6 hpf. Embryos were cultured under normal conditions (A and B) and PJ-34 (30 μ M) added 1 h before insemination or Sr^{2+} -activation (C and D). Signals of antibody for 5-methylcytosine (MetC) were colored with green. DNA counterstained with PI was colored in red (E–H). White circle represents the outlines of female (Fe) and male (M) pronuclei. Other PI signals represent DNA in the polar body (Pb). Values (percentage in parenthesis) represent frequency of staining patterns in each panel (A–D). EM observation of pronuclei in embryos at 6 hpf (I–P) and 15 hpf (Q–T) is shown in Fig. 3I–T. Rosette-like structures of electron-dense areas were detected in untreated female pronuclei at 6 hpf (arrowheads in M). The dense areas were increased by PARylation inhibition (arrowheads in O). Ambiguous outlines of pronuclear membrane were observed in PJ-34-treated embryos (arrows in O). Uncharacterized electron-dense structures were detected in female pronuclei with PARylation inhibition (white arrows and arrowheads in S). Rosette-like structures appeared in the male pronuclei of PJ-34-treated embryos (arrowheads in T). Bars represent 10 μ m (I–L) and 5 μ m (M–T). (For interpretation of color in Figure, the reader is referred to the web version of this article).

localization of Suz12, a histone methyltransferase, by PJ-34 may be related to the decrease of di-methylation of histone H3K9 and K27 in the female pronuclei. Suz12 is a component of PRC2/3/4, which regulates the repressive status of transcription by the methylation of histone H3K9 and H3K27 [34]. Our findings support the idea that Parp1 acts as a regulatory scaffold for the access of PRC2/3/4 to target DNA, because none of the components of the PRC2/3/4 complexes are DNA binding proteins. We previously observed Parp1, 2, 3, 6, 7, 8, 9, 12, 16 and Tans1 and 2 mRNAs are expressed in

the mouse oocytes [17]. Further analyses are needed to identify the responsible methyltransferases for histone H3K4 methylation, which are regulated by PARylation by particular PARP family member(s) during early stages of postfertilization development.

An additional conclusion of this finding is that PARylation regulates the epigenetic nonequivalence of the pronuclei in embryos (Fig. 4). The molecular mechanisms regulating the asymmetric DNA methylation of one-cell embryos are largely unknown. We were able to contribute to delineation of the mechanisms by show-

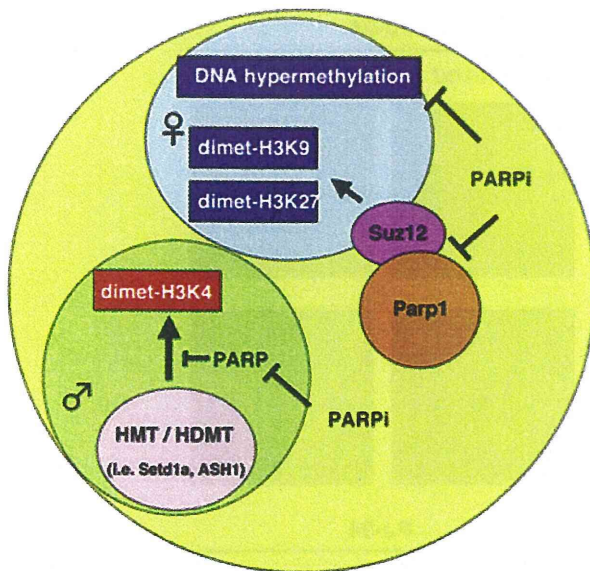


Fig. 4. Scheme of putative roles of PARylation in the chromatin dynamics of one-cell embryos. The Parp1-Suz12 complex may, in parts, regulate the H3K9 or H3K27 status of the female pronuclear genome. Hypermethylation status of female pronuclei may be regulated by the Dnmt1-Parp1 complex or other interactants of Parp1 including demethylases. On the other hand, H3K4 methylation of paternal pronuclei may be regulated by the interaction of PARP family member(s) and particular H3K4 methyltransferases present in oocytes through PARylation.

ing that PARylation is involved in the epigenetic regulation during early development in mice. PGC7/Stella-deficient eggs show similar defects in the protection of female pronuclei from DNA demethylation [35]. The nucleo-cytoplasmic transport of the responsible proteins appears to be important for the regulation of DNA methylation. The role of PARylation in DNA methyltransferase (DNMT) regulation is yet to be fully elucidated, although the interaction of DNMT1 with Parp1 and the indirect repression of DNMT1 activity by interacting with PAR have been suggested [36]. It is speculated that PARylation regulates the accessibility of DNMT or demethylase to DNA, in a manner mediated by chromatin remodeling. It is also of interest that PAR may participate in demethylation regulation by Gadd45a, involving base-excision repair, in which Parp1 and Parg also play important roles [37]. Our study provides a novel avenue for better understanding of establishment of chromatin organization through the histone codes, and DNA methylation with PARylation that may underlie at the beginning of zygotic development.

Acknowledgments

We would like to thank Hideki Ogino and for their technical assistance. We are grateful for Ryuzo Yanagimachi, Toshiaki Noce and Takashi Sugimura for discussion and suggestions. A. R. is a JSPS fellow.

This work was supported in part by a Grant-in-Aid from MEXT and the Third Term Comprehensive 10-Year Strategy for Cancer Control, National Cancer Center Research.

Appendix A. Supplementary data

Supplementary data associated with this article can be found, in the online version, at <http://dx.doi.org/10.1016/j.bbrc.2013.03.074>.

References

- [1] T. Sugimura, M. Miwa, Poly(ADP-ribose): historical perspective, *Mol. Cell Biochem.* 138 (1994) 5–12.
- [2] V. Schreiber, F. Dantzer, J.C. Ame, G. de Murcia, Poly(ADP-ribose): novel functions for an old molecule, *Nat. Rev. Mol. Cell Biol.* 7 (2006) 517–528.
- [3] D. D'Amours, S. Desnoyers, I. D'Silva, G.G. Poirier, Poly(ADP-ribosylation) reactions in the regulation of nuclear functions, *Biochem. J.* 342 (1999) 249–268.
- [4] A.J. Gottschalk, G. Timinszky, S.E. Kong, et al., Poly(ADP-ribosylation) directs recruitment and activation of an ATP-dependent chromatin remodeler, *Proc. Natl. Acad. Sci. USA* 106 (2009) 13770–13774.
- [5] M. Rouleau, R.A. Aubin, G.G. Poirier, Poly(ADP-ribosyl)ated chromatin domains: access granted, *J. Cell Sci.* 117 (2004) 815–825.
- [6] G. Timinszky, S. Till, P.O. Hassa, et al., A macrodomain-containing histone rearranges chromatin upon sensing PARP1 activation, *Nat. Struct. Mol. Biol.* 16 (2009) 923–929.
- [7] R. Krishnakumar, M.J. Gamble, K.M. Frizzell, et al., Reciprocal binding of PARP-1 and histone H1 at promoters specifies transcriptional outcomes, *Science* 319 (2008) 819–821.
- [8] H.L. Liu, K.T. Hara, F. Aoki, Role of the first mitosis in the remodeling of the parental genomes in mouse embryos, *Cell Res.* 15 (2005) 127–132.
- [9] C. Bouniol, E. Nguyen, P. Debey, Endogenous transcription occurs at the 1-cell stage in the mouse embryos, *Exp. Cell Res.* 218 (1995) 57–62.
- [10] C.C. Henery, M. Miranda, M. Wiekowski, et al., Repression of gene expression at the beginning of mouse development, *Dev. Biol.* 169 (1995) 448–460.
- [11] R.M. Schultz, Regulation of zygotic gene activation in the mouse, *BioEssay* 15 (1993) 531–538.
- [12] W. Tadros, H.D. Lipshitz, The maternal-to-zygotic transition: a play in two acts, *Development* 136 (2009) 3033–3042.
- [13] R.M. Schultz, The molecular foundations of the maternal to zygotic transition in the preimplantation embryo, *Hum. Reprod. Update* 8 (2002) 323–331.
- [14] D.W. McKay, H.J. Clarke, The ability to organize sperm DNA into functional chromatin is acquired during meiotic maturation in murine oocytes, *Dev. Biol.* 186 (1997) 73–84.
- [15] G.T. Williams, S. Shall, C.C. Ford, NAD turnover during early development of *Xenopus laevis*, *Biochim. Biophys. Acta* 762 (1983) 272–280.
- [16] D. Epel, The initiation of development at fertilization, *Cell Differ. Dev.* 29 (1990) 1–12.
- [17] T. Osada, H. Ogino, T. Hino, et al., PolyADP-ribosylation is required for pronuclear fusion during postfertilization in mice, *PLoS One* 5 (2010) e12526.
- [18] T. Osada, M. Masutani, PolyADP-ribosylation in postfertilization and genome reprogramming: implications for carcinogenesis, in: Gomes, A.D.S. Gomes (Eds.), *Polymerization*, InTech, New York, 2012, 10.5772/46097.
- [19] M. Masutani, H. Suzuki, N. Kamada, et al., Poly(ADP-ribose) polymerase gene disruption conferred mice resistant to streptozotocin-induced diabetes, *Proc. Natl. Acad. Sci. USA* 96 (1999) 2301–2304.
- [20] Y. Toyoda, M. Yokoyama, T. Hoshi, Studies on the fertilization of mouse eggs in vitro, *J. Anim. Reprod.* 16 (1971) 147–151.
- [21] T. Osada, A. Toyoda, S. Moisyadi, et al., Production of inbred and hybrid transgenic mice carrying lathe (>200 kb) foreign DNA fragments by intracytoplasmic sperm injection, *Mol. Reprod. Dev.* 72 (2005) 329–335.
- [22] M.C. Summers, L.K. McGinnis, J.A. Lawitts, et al., IVF of mouse ova in a simplex optimized medium supplemented with amino acids, *Hum. Reprod.* 15 (2000) 1791–1801.
- [23] W.K. Whitten, J.D. Biggers, Complete development in vitro of the pre-implantation stages of the mouse in a simple chemically defined medium, *J. Reprod. Fertil.* 17 (1968) 399–401.
- [24] C. Simerly, G. Schatten, Techniques for localization of specific molecules in oocytes and embryos, *Methods Enzymol.* 225 (1993) 516–553.
- [25] E. Perkins, D. Sun, A. Nguyeb, et al., Novel inhibitors of poly(ADP-ribose) polymerase/PARP1 and PARP2 identified using a cell-based screen in yeast, *Cancer Res.* 61 (2001) 4175–4183.
- [26] F.E. Erfurth, R. Popovic, J. Grembecka, et al., MLL protects CpG clusters from methylation within the Hoxa9 gene, maintaining transcript expression, *Proc. Natl. Acad. Sci. USA* 105 (2008) 7517–7522.
- [27] T. Vaissiere, C. Swan, Z. Herceg, Epigenetic interplay between histone modification and DNA methylation in gene silencing, *Mutat. Res.* 659 (2008) 40–48.
- [28] W. Mayer, A. Niveleau, J. Walter, et al., Demethylation of the zygotic paternal genome, *Nature* 402 (2000) 501–502.
- [29] D. Quenet, V. Gasser, L. Fouillen, et al., The histone subcode: poly(ADP-ribose) polymerase-1 (Parp-1) and Parp-2 control cell differentiation by regulating the transcriptional intermediary factor TIF beta and heterochromatin protein HP1alpha, *FASEB J.* 22 (2008) 3853–3865.
- [30] T. Boulikas, Poly(ADP-ribosylated) histones in chromatin replication, *J. Biol. Chem.* 265 (1980) 14638–14647.
- [31] A. Huber, P. Bai, M. de Murcia, et al., PARP-1, PARP-2 and ATM in the DNA damage response: functional synergy in mouse development, *DNA Repair* 3 (2004) 1103–1108.
- [32] G.G. Poirier, G. de Murcia, J. Jongstra-Bilen, et al., Poly(ADP-ribosylation) of polynucleosomes causes relaxation of chromatin structure, *Proc. Acad. Natl. Sci. USA* 79 (1982) 3423–3427.
- [33] A. Tulin, A. Spradling, Chromatin loosening by poly(ADP-ribose) polymerase (PARP) at *Drosophila* puff loci, *Science* 299 (2003) 560–562.

- [34] R. Cao, Y. Zhang, SUZ12 is required for both the histone methyltransferase activity and the silencing function of the EED-EZH2 complex, *Mol. Cell* 2 (2004) 57–67.
- [35] T. Nakamura, Y. Arai, H. Umehara, et al., PGC/Stella protects against demethylation in early embryogenesis, *Nat. Cell Biol.* 9 (2007) 64–71.
- [36] P. Caiafa, T. Guastafierro, M. Zampieri, Epigenetics: poly(ADP-ribosyl)ation of PARP-1 regulates genomic methylation patterns, *FASEB J.* 23 (2009) 672–678.
- [37] G. Barreto, A. Schafer, J. Marhold, et al., Gadd45a promotes epigenetic gene activation by repair-mediated DNA demethylation, *Nature* 445 (2007) 671–675.

Induction of Cancerous Stem Cells during Embryonic Stem Cell Differentiation^{*[5]}

Received for publication, April 17, 2012, and in revised form, August 30, 2012. Published, JBC Papers in Press, September 7, 2012, DOI 10.1074/jbc.M112.372557

Hiroaki Fujimori^{†‡§}, Mima Shikanai[§], Hirobumi Teraoka[§], Mitsuko Masutani[†], and Ken-ichi Yoshioka^{†§1}

From the [†]Division of Genome Stability Research, National Cancer Center Research Institute, 5-1-1 Tsukiji, Chuo-ku, Tokyo 104-0045, Japan and the [§]Department of Pathological Biochemistry, Medical Research Institute, Tokyo Medical and Dental University, 2-3-10 Kandasurugadai, Chiyoda-ku, Tokyo 101-0062, Japan

Background: Cancer stem cells are responsible for tumorigenesis; however, the developmental process is poorly understood.

Results: Differentiating stem cells in aberrant environments are subjected to carcinogenic stress, leading to genomic instability, mutation inductions, and cellular transformation with stemness characteristics.

Conclusion: Aberrant environment for differentiation risks cancerous stem cell development.

Significance: This is the first report showing normal stem cell transformation into malignant counterparts and their process.

Stem cell maintenance depends on their surrounding micro-environment, and aberrancies in the environment have been associated with tumorigenesis. However, it remains to be elucidated whether an environmental aberrancy can act as a carcinogenic stress for cellular transformation of differentiating stem cells into cancer stem cells. Here, utilizing mouse embryonic stem cells as a model, it was illustrated that environmental aberrancy during differentiation leads to the emergence of pluripotent cells showing cancerous characteristics. Analogous to precancerous stages, DNA lesions were spontaneously accumulated during embryonic stem cell differentiation under aberrational environments, which activates barrier responses such as senescence and apoptosis. However, overwhelming such barrier responses, piled-up spheres were subsequently induced from the previously senescent cells. The sphere cells exhibit aneuploidy and dysfunction of the *Arf-p53* module as well as enhanced tumorigenicity and a strong self-renewal capacity, suggesting development of cancerous stem cells. Our current study suggests that stem cells differentiating in an aberrational environment are at risk of cellular transformation into malignant counterparts.

A tumor consists of a heterogeneous cell mass in which only a small portion of the malignant cells, *i.e.* cancer stem cells (CSCs),² are responsible for tumor initiation and propagation (1). In fact, CSCs identified in a variety of tumors demonstrate a

capacity for self-renewal and differentiation, which is shared by normal stem cells (2). Although cancer stem-like cells can be induced from stem/progenitor as well as differentiated cells by oncogene overexpression (3, 4), it remains unclear how CSCs spontaneously develop.

In the initial stages of carcinogenesis cells accumulate DNA replication stress-associated lesions that are induced by aberrant growth acceleration or oncogene activation, resulting in the activation of barrier reactions for carcinogenesis such as cell cycle arrest, senescence, and apoptosis (5, 6). These cellular responses illustrate the competing forces of cancer progression and prevention. Genomic instability is invariably accompanied with these stages of cancer development (6, 7). Analogously, mouse embryonic fibroblasts (MEFs) can escape senescence and exhibit immortality through accumulation of DNA replication stress-associated lesions under continuous growth acceleration, which accompanies genomic instability (8) and *Arf/p53* mutations (9). However, unlike CSCs, immortalized MEFs show neither tumorigenicity nor stemness characteristics (10).

The difference between immortal MEFs and CSCs underlies the properties of stemness characteristics. In addition to the expression of undifferentiated marker genes, both somatic stem cells and CSCs show sphere-formation abilities and heightened expression of the ATP binding cassette transporter and glycolysis dependence (11, 12). Importantly, whereas these properties are widely observed in stem cells, including embryonic stem cells (ESCs) (13–16), immortal MEFs do not acquire such properties during immortalization. Unlike immortal MEFs, CSCs share specific profiles of cell-surface antigens with somatic stem cells (11). However, like immortal MEFs, CSCs also show genomic instability and mutations, which are unshared characteristics with normal stem cells (17).

The existing body of literature on stem cells suggests that carcinogenesis can be initiated in somatic stem cells when the cells are subjected to the same conditions of stress that induce MEF immortalization. However, this challenges the idea of stem cell homeostasis, which is strongly protected by niche environments from the induction of genomic instability and

* This work was supported, in whole or in part, by Ministry of Education, Culture, Sports, Science, and Technology of Japan KAKENHI (20770136, 20659047), Grant-in-aid and the Third Term Comprehensive 10-Year Strategy for Cancer Control (10103833), and the National Cancer Center Research and Development Fund (23-C-10).

[5] This article contains supplemental Tables 1 and 2 and Figs. S1–S5.

¹ To whom correspondence should be addressed. Tel.: 81-3-3542-2511; Fax: 81-3-3543-9305; E-mail: kyoshiok@ncc.go.jp.

² The abbreviations used are: CSC, cancer stem cell; MEF, mouse embryonic fibroblast; ESC, embryonic stem cell; EB, embryoid body; NBS, newborn bovine serum; ABS, adult bovine serum; HU, hydroxyurea; iLC, induced immortal-like cell; NCS, neocarzinostatin; cGC, continuously growing cell; PARP, poly(ADP-ribose) polymerase; KSR, knockout serum replacement; LIF, mouse leukemia inhibitory factor.

Differentiating Stem Cell Transformation

transformation (18). In agreement with this argument, stem cells injected into heterotopic sites are strongly implicated in tumorigenesis, in association with environmental aberrancies for stem cell maintenance (19). Further supporting the notion of stem cell tumorigenicity in aberrant environments, embryonal carcinomas were developed from xenografts of inner cell masses from mouse blastocyst and derailed primordial germ cells from the migration track (20, 21). Moreover, a recent study suggested that oncogenesis could be triggered by a niche disruption, resulting in disordered differentiation (22).

Taken together with a report showing stem cell niche dysfunction as a result of aging (23), these studies motivated the hypothesis that differentiating stem cells can become CSCs upon exposure to carcinogenic stress in a process analogous to MEF immortalization.

MATERIALS AND METHODS

Cell Culture—Culture of mouse ESCs and embryoid body (EB) formation assays were performed as previously described (24). For differentiation, cloned ESCs maintained with Knock-Out Serum Replacement (Invitrogen) and ESGRO (mouse leukemia inhibitory factor (LIF); Millipore, Billerica, MA) were cultured in three kinds of medium consisting of Iscove's modified Dulbecco's medium (Invitrogen) supplemented with FBS (Invitrogen), newborn bovine serum (NBS; Sigma), or adult bovine serum (ABS; Invitrogen) at 20%. The piled-up spheres were stained by crystal violet (Sigma), and the number of spheres was counted. Populations at P6 + 14 days were harvested by employing 0.25% trypsin-EDTA (Invitrogen) and then cultured in each medium for further experiments. All the following experiments were performed using bulk populations without cloning. Primary MEF immortalization assays were performed as previously described (8). For detection of the phenotype with an abnormal p53 pathway, each population was cultured in medium containing hydroxyurea (HU) as previously described (25). Sphere formation assay was performed as previously described (26) with a little modification. Briefly, CD133-positive and -negative populations were seeded to NBS-med containing methylcellulose 4000 (Wako, Tokyo, Japan) for 4 days. For detection, spheres were attached to culture dishes and were stained by crystal violet after 2 days of attachment (Sigma).

β -Galactosidase Activity Detection— β -Galactosidase activity was detected as previously described (27). Briefly, cultured cells were fixed with 4% formaldehyde and then incubated in staining buffer (1 mg/ml 5-bromo-4-chloro-3-indolyl- β -D-galactopyranoside (X-gal), 5 mM $K_3Fe(CN)_6$, 5 mM $K_4Fe(CN)_6$, and 2 mM $MgCl_2$ in PBS).

Reverse Transcription-Polymerase Chain Reaction—RT-PCR and quantified RT-PCR were performed as described (24). Briefly, total RNA was extracted from cultured cells with an RNeasy kit (Qiagen, Tokyo, Japan) and treated with DNase I (Promega, Tokyo, Japan). cDNAs were synthesized from 1 μ g of total RNA using Super Script III first-strand synthesis system (Invitrogen). Ampli Taq Gold PCR Master Mix (Invitrogen) or Power SYBR Green PCR Master Mix (Invitrogen) was employed for PCR reaction. The primer list is described in supplemental Table 1.

Antibodies, Immunostaining and Western Blotting—The antibodies used are listed in supplemental Table 2. Immunostaining and Western blot analysis were performed as previously described (8). Briefly, for Western blotting, proteins were transferred onto a nitrocellulose membrane and probed with appropriate primary antibodies. The membrane was incubated with corresponding secondary antibodies conjugated with horseradish peroxidase, and the antigen-antibody complex was visualized by Immobilon Western (Millipore). For immunostaining, cells were fixed with formalin and then treated with Triton X-100. After blocking with serum, they were incubated with each primary antibody and then detected with fluorescent secondary antibodies.

Chromosomal Instability Detection—Giemsa staining and flow cytometric analysis were performed as previously described (8). Briefly, mitotic cells prepared by nocodazole treatment were hypotonically swollen with 75 mM KCl and then fixed with Carnoy's solution (75% methanol, 25% acetic acid). They were stained with 4% Giemsa (Merck) solution.

Apoptosis Detection Assay—Terminal deoxynucleotidyltransferase-mediated dUTP-biotin nick-end labeling (TUNEL) was performed with the *in situ* Apoptosis Detection kit (Takara Bio, Otsu, Japan). The TUNEL-positive cells were detected by FACSCalibur HG (BD Biosciences). The sub- G_1 population was quantified as previously described (28).

Detection of p53 Mutation—The p53 transcripts from each population were amplified from the cDNA from each population and cloned using the pGEM-Easy vector system (Promega), and then the clones were sequenced by an ABI PRISM 3700 DNA analyzer (Invitrogen).

Tumor Formation Assay—For the tumor formation assay, 10^6 cells suspended in 100 μ l of serum-free medium were mixed with an equal-volume of growth factor-reduced Matrigel (BD Biosciences) and injected subcutaneously into NOD.CB17-Prkdc^{scid}/J (NOD-SCID) mice. Tumor weight was measured 4 weeks after injection. Tumors were dissolved by dispase (Invitrogen) in part, and total RNA was extracted.

Isolation of CD133-positive Cells—CD133 positive fractions of induced immortal-like cells (iICs) in NBS-med were isolated by a magnetic bead cell sorting or fluorescence activated cell sorting (FACS) technique as previously described (24, 29). Briefly, for magnetic bead cell sorting, Dynabeads (Invitrogen) were coated with CD133 antibody (eBioscience). The beads/antibody complexes were incubated with cells, then the CD133-positive fraction was collected by a magnetic particle concentrator (Invitrogen). RNA was extracted from CD133-positive and -negative populations and subjected to RT-PCR. For FACS, cells incubated with CD133 antibody conjugated with Alexa Fluor 488 were sorted by FACS Aria II system (BD Biosciences). CD133-positive and negative fractions were subjected to sphere formation assay. Details of employed antibodies are described in supplemental Table 2.

Chemical Treatment of Differentiating Cells—The differentiating cells 1 day after passage 3 in ABS medium were treated with 25, 75, or 200 ng/ml neocarzinostatin (NCS). After 1 day, cells were passaged with NCS(+) medium. After 3 days, medium was changed to NCS(-) medium. This procedure is illustrated in Fig. 4E.